East European Journal of Physics. 4. 274-283 (2025)
DOI:10.26565/2312-4334-2025-4-25 ISSN 2312-4334

PUSHING EFFICIENCY LIMITS: SCAPS-BASED ANALYSIS OF GaAs AND BAs SOLAR CELLS FOR NEXT-GENERATION PHOTOVOLTAICS

Merad Laarej*, Mama Bouchaour§, Imane Bouazzaoui
University of Tlemcen, Faculty of Sciences, Department of Physics, Unity of Research "Materials and Renewable Energies", URMER BP : 119, Tlemcen, Nouveau Pôle, Mansourah, 13000, Algeria
**Corresponding Author e-mail: la_merad@yahoo.fr and §bouchaour.m@gmail.com*
Received May 2, 2025; revised July 8, 2025; accepted November 3, 2025

The present study utilizes SCAPS software to simulate and analyze the semiconductor materials gallium arsenide (GaAs) and boron arsenide (BAs) for photovoltaic applications. We outline the methodology, emphasizing critical factors considered during simulation. The performance of solar cells is investigated through quantum efficiency and photovoltaic performance curves. Additionally, the observed trends, key differences between GaAs and BAs, and their implications for advancing high-efficiency solar cells are discussed.
Keywords: *GaAs; BAs; Photovoltaic; SCAPS Software; Conversion Efficiency (η)*
PACS: 88.40.hj

1. INTRODUCTION

Gallium arsenide (GaAs) is a prominent material in the photovoltaic industry due to its direct bandgap and remarkable electronic transport properties. Its ability to efficiently absorb sunlight and convert photonic energy into electricity makes it a preferred material for high-performance solar cells.

Boron arsenide (BAs), while still in the development phase, has garnered attention for its promising properties in photovoltaic applications. With a wider bandgap compared to GaAs, BAs is potentially better suited for capturing high-energy photons in the solar spectrum. However, its practical implementation in photovoltaic cells remains a technical challenge.

The article solves the physical problem of designing next-generation solar cells by elucidating the trade-offs between light absorption, charge transport, recombination losses, and thermal stability, thereby guiding the practical optimization of both GaAs- and BAs-based devices for enhanced, stable photovoltaic performance.

This comprehensive approach not only advances our theoretical understanding but also has direct implications for developing efficient, robust solar cell technologies for real-world applications.

2. STATE OF THE ART FOR THE ANALYSIS OF SOLAR CELL PERFORMANCE

In recent years, high-efficiency solar cells have predominantly relied on III-V semiconductors, such as GaAs (Gallium Arsenide), due to their:

- Direct bandgap (\~1.42 eV).
- High carrier mobility.
- Excellent performance under high radiation and temperature conditions (ideal for aerospace and concentrator photovoltaics).

To push efficiency beyond 30%, researchers have:

- Optimized multi-junction structures combining materials of varying bandgaps.
- Employed advanced transport layers (e.g., InGaP, AlGaInP).
- Used SCAPS-1D and other simulation tools to optimize layer thickness, doping, and interface quality.

Studies like those by [1] achieved efficiencies up to 30.88% in GaAs-based solar cells using complex heterojunctions. Other works, such as like [2], have used using pin-type GaAs cells in SCAPS simulations, reached efficiencies around 28.5%.

On the other hand, Boron Arsenide (BAs) is an emerging semiconductor, predicted to offer:

- A wide bandgap (\~2.45 eV).
- Exceptional thermal conductivity.
- High ambipolar mobility.

These properties are promising for thermophotovoltaic and space applications, but its use in actual solar cells remains mostly theoretical or simulation-based due to fabrication challenges.

3. STRUCTURES STUDIED

To ensure an accurate comparison, the study evaluates two heterostructures based on BAs and GaAs under identical conditions (Figure 1). Both structures incorporate copper oxide (CuO) as the hole transport layer, facilitating

Cite as: M. Laarej, M. Bouchaour, I. Bouazzaoui, East Eur. J. Phys. 4, 274 (2025), https://doi.org/10.26565/2312-4334-2025-4-25

the collection of positive charge carriers generated in the photovoltaic device's active layer. Tungsten disulfide (WS2) serves as the electron transport layer, aiding in the collection of negative charge carriers.

A fluorine-doped tin oxide (FTO) layer is utilized as a transparent electrode in both configurations. This layer reduces voltage losses and enhances the efficiency of solar energy conversion into electrical power by providing a conductive interface between the active layer and the external circuit. This setup allows for a comprehensive comparison of the photovoltaic potential of GaAs and BAs under controlled and comparable conditions.

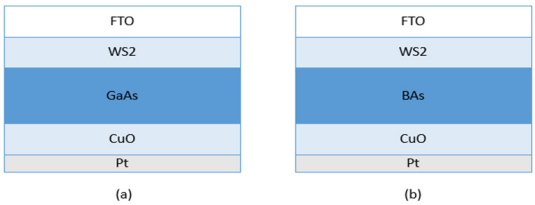

Figure 1. Structure of GaAs-based solar cells (a), BAs-based solar cells (b)

3.1. Physical and Optical Parameters of the Studied Cells

Table 1 displays the physical and optical parameters used in the SCAPS-1D simulations. The thickness of the CuO, WS2, and FTO layers were set to 0.1 µm, 0.2 µm, and 0.015 µm, respectively, based on typical values reported for thin-film solar cell devices. The band gap of GaAs (1.42 eV) was taken from a standard semiconductor reference, while the band gap of BAs (2.45 eV) was obtained from theoretical calculations by Wentzcovitch and Cohen. The electron affinity and dielectric permittivity values for BAs were taken from Bushick et al. The electron mobility of GaAs was set to 8800 cm²/Vs, representing a high-quality single-crystal value, while the mobility of BAs was taken from experimental measurements on synthesized crystals.

Table 1. Parameters of the materials used in the simulation of the examined cells

Parameters	CuO	GaAs	WS2	FTO	BAs
Thickness (μm)	0.1	Variable	0.2	0.015	Variable
Band gap energy (eV)	2.17	1.42	1.870	3.5	1.46 [1] [2]
Electron affinity (eV)	3.2	4.07	4.3	4	4.495 [3]
Dielectric permittivity (relative)	7.110	13.8	11.9	9	9.02 [3]
Effective density of states of the conduction band (cm^{-3})	2.02×10^{17}	2.2×10^{18}	1×10^{17}	2×10^{18}	3.01×10^{17}[3]
Effective density of states of the valence band (cm^{-3})	1.1×10^{19}	1.8×10^{19}	2.4×10^{19}	1.8×10^{19}	5.58×10^{18} [3]
Electron mobility (cm^2/Vs)	200	8800 [4]	260	20	1400
Mobility of holes (cm^2/Vs)	81	400	51	10	2100
Doping concentration of donors (cm^{-3})	0	0	10^{17}	10^{19}	0
Concentration of acceptor doping (cm^{-3})	10^{16}	variable	0	0	variable
References	[5]	[6]	[7][8]	[9]	[10]

3.2. Evaluation of the simulated structures' baseline performance

The simulation results obtained using simplified models, which exclude variations in thickness, doping levels, and defect density, are presented in Table 2. This approach allows for a direct comparison of the baseline photovoltaic characteristics of each structure, providing an assessment of their initial performance under comparable and idealized conditions.

Table 2. Results of basic structure simulations

Structures	V_{oc} (V)	J_{sc} (mA/cm^2)	FF (%)	ŋ (%)
Pt/CuO/GaAs/WS2/FTO	1.0997	24.3669	83.71	22.43
Pt/CuO/BAs/WS2/FTO	1.2270	23.2075	83.91	23.89

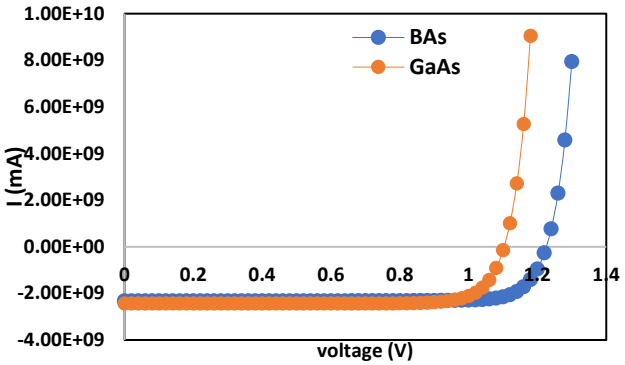

Figure 2. Variation of the current density I as a function of the voltage V for both GaAs and BAs

The results in Table 2 indicate that while GaAs achieved a slightly higher short-circuit current, BAs compensated with a superior fill factor, leading to greater overall photovoltaic conversion efficiency in this configuration. This suggests that, for this specific application, BAs may outperform GaAs in terms of charge management and minimizing internal losses.

Figure 2, present a current-voltage (I-V) characteristic comparison between two semiconductor materials**:** BAs (Boron Arsenide) and GaAs (Gallium Arsenide)**.** In reverse bias, both materials exhibit very low leakage current, slightly lower for BAs,

indicating high-quality junctions. Under forward bias, GaAs starts conducting at a lower voltage (~0.95 V), while BAs requires a higher threshold (~1.05 V), suggesting a wider bandgap for BAs. The current rises more sharply for GaAs, reflecting better carrier injection at low voltages [11]. However, BAs demonstrates a more stable behavior, with lower recombination losses. Therefore, GaAs performs better at low voltages, while BAs shows greater stability and potential for high-voltage or harsh-environment applications.

III. Comparative Study of GaAs and BAs-Based Solar Cells

This comparative study examines the performance of GaAs-based solar cells, a well-established material, and BAs, a promising emerging material for photovoltaic applications. By varying the active layer thickness, doping levels, and accounting for defects, we evaluate their effects on photovoltaic performance to gain deeper insights into the strengths and limitations of these materials in solar energy applications.

III.1. Effect of the active layer thickness

We explore thicknesses ranging from 0.25 to 3 µm to determine the optimal level for light absorption, ensuring maximum efficiency. Additionally, we pinpoint the critical threshold beyond which efficiency declines as thickness increases, offering valuable insights for designing high-performance solar cells while minimizing material consumption.

III.1.1. Variation of V_{oc} as a function of thickness

Figure 3 illustrates two distinct trends, one for GaAs and the other for BAs, highlighting the impact of active layer thickness on the open-circuit voltage (V_{oc}) in solar cells. Notably, the V_{oc} decreases as the active layer thickness increases for both materials. Interestingly, however, the BAs curve consistently remains higher than that of GaAs at any given thickness.

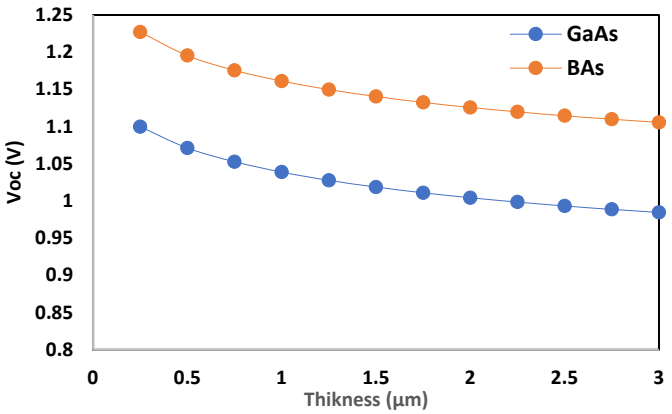

Figure 3. Variation of V_{oc} as a function of thickness

The decrease in V_{oc} with increasing active layer thickness can be explained as follows: As the thickness of the active layer increases, charge carriers (electrons and holes) must travel longer distances to reach the solar cell electrodes. This extended travel increases the likelihood of recombination before the carriers reach the electrodes, thereby reducing the voltage generated by the cell.

Increasing the active layer thickness can lead to greater light absorption within the layer itself, reducing the amount of light that reaches the p-n junction and thereby lowering the voltage generated by the cell. Additionally, BAs, with its wider bandgap compared to GaAs, requires higher energy for electrons and holes to recombine [12]. This characteristic reduces charge carrier recombination, resulting in a higher V_{oc} for BAs compared to GaAs.

III.1.2. Variation of J_{sc} as a function of thickness

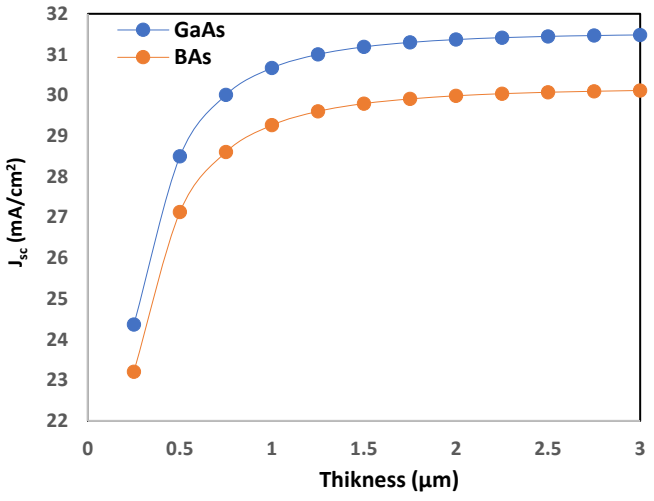

Figure 4. J_{sc} vs with thickness

Figure 4 presents two different curves, one for GaAs and one for BAs, illustrating the relationship between short-circuit current density (J_{sc}) and active layer thickness in solar cells. For both materials, J_{sc} increases as the active layer thickness grows. However, for GaAs, this increase is more pronounced between 0.25 µm and 1.5 µm, after which the Jsc begins to rise marginally or stabilizes. Notably, the GaAs curve consistently remains above the BAs curve for any given thickness.

The increase in Jsc with active layer thickness is due to more photons being absorbed and converted into electron-hole pairs as the layer becomes thicker. Beyond a certain thickness, light absorption reaches a saturation point, causing Jsc to stabilize as additional material no longer significantly enhances photon absorption.

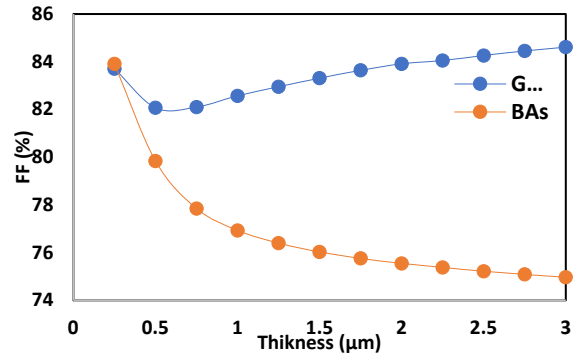

Figure 5. Variation of fill factor (FF) as a function of thickness

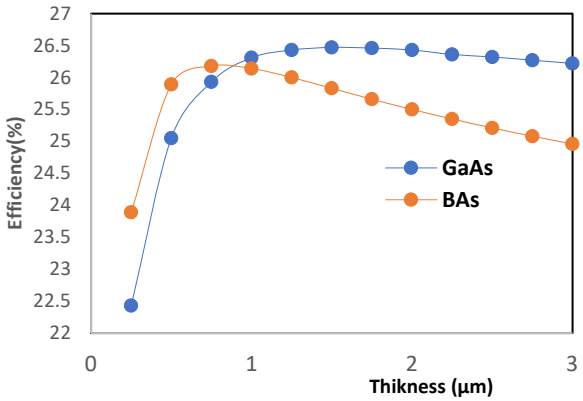

Figure 6. Variation of efficiency as a function of thickness

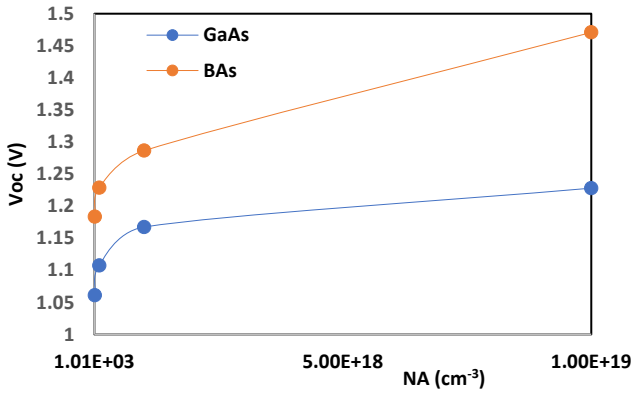

Figure 7. Variation of V_{oc} as a function of p-type doping

The GaAs curve remains higher than the BAs curve throughout due to GaAs's superior electron mobility, which facilitates faster electron transport and minimizes recombination losses [13]. Consequently, while both materials exhibit an increase in J_{sc} with thickness, GaAs consistently generates higher current for a given thickness, benefiting from its more efficient charge transport properties.

Figure 5 illustrates two graphs showing the fill factor (FF) of GaAs and BAs as a function of active layer thickness in a solar cell. Notably, the FF initially drops to around 0.5 µm and then gradually increases as the thickness continues to rise. This behavior can be attributed to rising resistive losses at lower thicknesses, which initially reduce the FF. However, beyond this point, improved charge carrier separation and better control of recombination processes offset these losses, leading to an increase in the FF.

In contrast, the fill factor of BAs shows a significant decline with increasing active layer thickness, unlike GaAs. This reduction in FF suggests a potential decline in material quality as the active layer thickens, which may be attributed to an increase in charge carrier recombination. This difference highlights the challenges associated with maintaining optimal performance in BAs-based solar cells as layer thickness increases.

III.1.3. Variation of the efficiency (η) versus the thickness

Figure 6 depicts the variation in efficiency as a function of active layer thickness. For GaAs, efficiency increases within the range of 0.25 to 1.75 µm, reflecting improved light absorption and enhanced charge carrier management. Beyond this range, efficiency either stabilizes or slightly decreases, indicating that most incident photons have already been absorbed, and further gains are limited to marginal effects.

In contrast, BAs shows a similar trend to GaAs within the range of 0.25 to 0.75 µm. However, beyond this point, the efficiency decreases more significantly [14]. This pronounced decline suggests the presence of adverse factors such as non-radiative recombination or structural imperfections, which diminish the overall efficiency of the solar cell.

III. 2 Doping Effect of the Active Layer

We analyze the impact of varying doping concentrations, ranging from low levels ($1\times10^{14} – 1\times10^{15}$) to high levels ($1\times10^{18} – 1\times10^{19}$), on critical parameters such as J_{sc}, V_{oc}, FF, and PCE. This analysis enables the identification of optimal doping levels to maximize the performance and efficiency of solar cells.

III.2.1. Variation of V_{oc} as a function of doping in the active layer

Figure 7, presents two graphs illustrating the open-circuit voltage (V_{oc}) as a function of p-type doping concentration for GaAs and BAs materials in a solar cell. V_{oc} increases with higher doping levels for both materials, but at every doping level, the BAs curve consistently remains above that of GaAs.

As the p-type doping concentration rises, the number of holes in the active layer increases [15]. This higher hole density reduces the depletion zone width within the p-n junction, decreasing charge carrier recombination losses in this region. Consequently, the open-circuit voltage (V_{oc}) is enhanced, improving the overall performance of the solar cell.

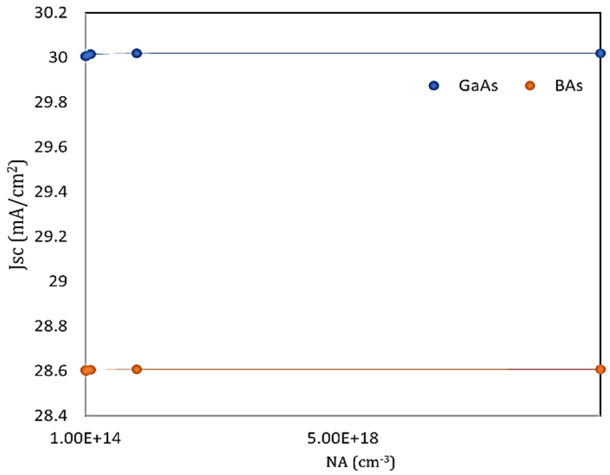

Figure 8. Variation of J_{sc} versus p-type doping

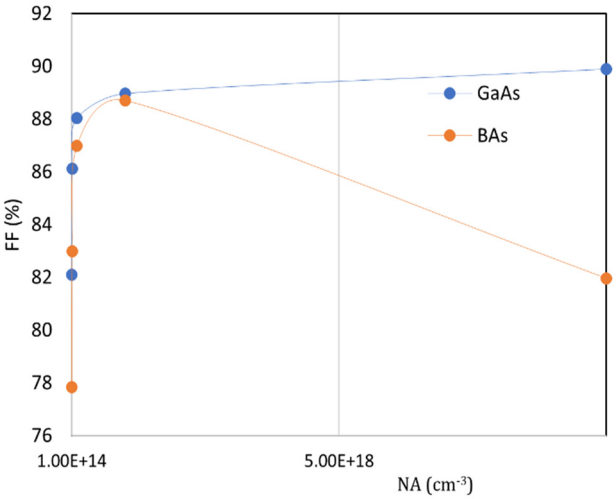

Figure 9. Variation of the form factor (FF) as a function of P-type doping

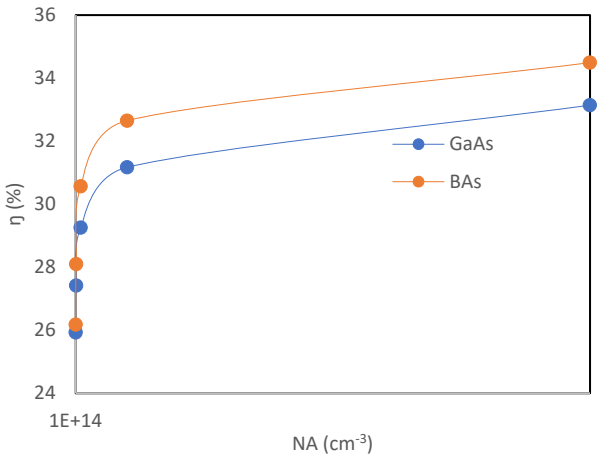

Figure 10. Variation of (ŋ) as a function of P doping

III.2.2. Variation of J_{sc} as a function of doping in the active layer

Figure 8 illustrates the variation of short-circuit current density (J_{sc}) for GaAs and BAs as a function of p-type doping concentration (NA). Despite an increase in NA from 1×10^{14} to 1×10^{19} cm³, the Jsc for GaAs remains nearly constant at approximately 30 mA/cm², while for BAs, it remains steady at around 28.6 mA/cm² across the same doping range [11].

This stability indicates that the generation and accumulation of charge carriers are not significantly affected by higher doping concentrations. The consistency suggests that the solar cells are already optimized for photon absorption and charge carrier collection, and additional doping does not notably enhance their performance within this range.

III.2.3. Variation of the fill factor (FF) as a function of doping of the active layer

Figure 9 illustrates the variation in the fill factor (FF) as a function of p-type doping concentration for GaAs and BAs. In both materials, increasing the p-type doping concentration generally enhances the FF, indicating that charge carrier mobility in these semiconductors improves with higher doping levels.

For GaAs, the FF shows a steady increase with rising doping concentration, suggesting consistent improvements in conductivity. In contrast, BAs initially exhibits a significant increase in FF; however, at very high doping concentrations, the FF begins to decline. This decline may result from saturation effects or increased recombination phenomena, indicating a threshold beyond which further doping becomes detrimental to the material's performance.

III.2.4. Variation of efficiency (ŋ) as a function of doping of the active layer

Figure 10 presents two graphs showing the efficiency of GaAs and BAs solar cells as a function of p-type doping concentration. For both materials, efficiency increases with higher doping levels. In GaAs, this increase is particularly pronounced, with the power conversion efficiency (PCE) rising from 27.42% to 33.14% as doping concentrations increase from 1×10^{14} to 1×10^{18}. This improvement reflects enhanced efficiency in converting light energy into electricity due to increased doping. The higher concentration of positive charge carriers (holes) resulting from p-type doping improves charge separation, thereby facilitating more efficient energy conversion.

Similarly, BAs shows an efficiency increase with higher doping levels, but the rise in PCE is more gradual, from 32.65% to 34.49% between doping concentrations of 1×10^{18} and 1×10^{19}. This trend suggests a potential saturation point, where further doping yields diminishing returns. This limitation could be attributed to effects such as charge carrier recombination or the saturation of available doping sites, indicating a practical upper limit to the benefits of p-type doping on photovoltaic conversion efficiency.

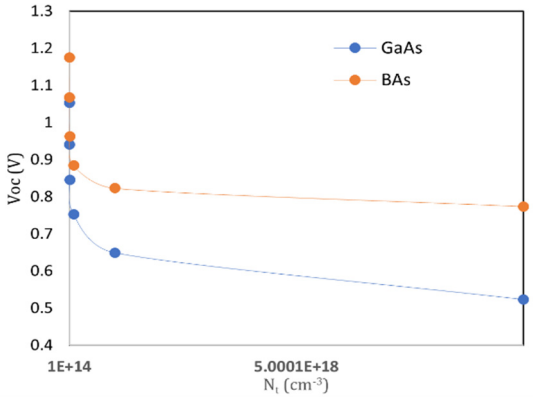

Figure 11. Variation of Voc as a function of defect density N_t

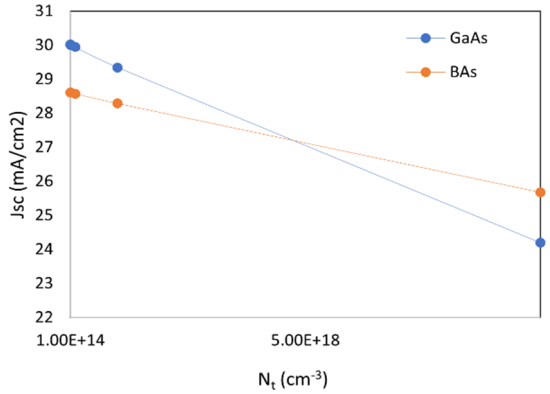

Figure 12. Variation of J_{sc} as a function of defect density N_t

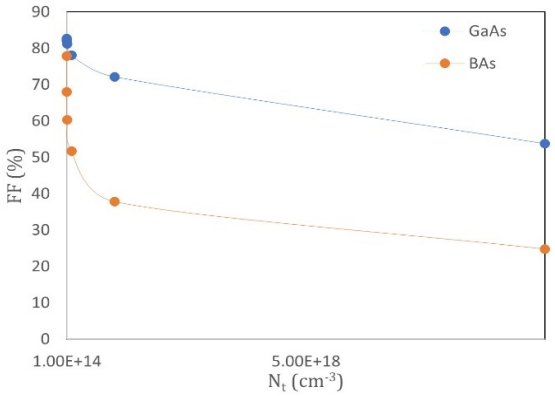

Figure 13. Variation of the fill factor (FF) as a function of defect density N_t

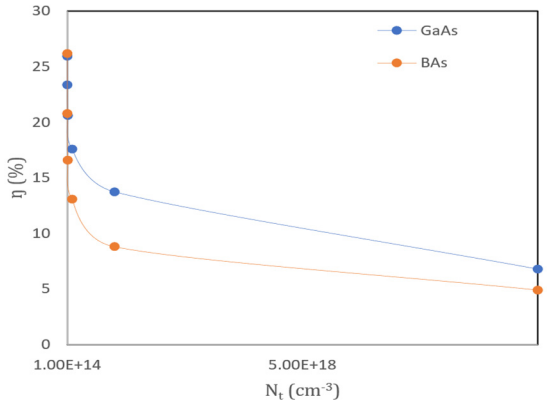

Figure 14. Variation of efficiency as a function of defect density Nt

III.2.5. Effect of defects in the active layer

Figure 11 illustrates the variation in the open-circuit voltage (V_{oc}) as a function of defect density N_t for GaAs and Bas. By examining a range of defect density values, we can assess their impact on the electrical characteristics of the solar cell. This analysis shall enable us to identify the optimal defect density, contributing to enhanced overall performance and efficiency of the solar cell.

A gradual decline in the open-circuit voltage (V_{oc}) is observed for both GaAs and BAs as the defect density in the crystalline layer increases. Initially, the decrease is mild, but it becomes more pronounced at higher defect levels.

Comparatively, while BAs may initially exhibit a slightly higher V_{oc} than GaAs, its drop at higher defect densities is more significant, indicating greater sensitivity to defects. This suggests that BAs may be more affected by disruptions in the crystalline structure.

For both materials, the decrease in V_{oc} aligns with the principle that defects disrupt the crystalline structure, reducing charge carrier mobility and ultimately impacting the open-circuit voltage.

III.2.6. Variation of short-circuit current density (Jsc) as a function of doping of the active layer

Figure 12 demonstrates that the short-circuit current density (J_{sc}) gradually decreases as the defect density (N_t) increases for both GaAs and BAs materials.

The decline in J_{sc} with increasing N_t is attributed to the rise in recombination centers within the material. These defects elevate the likelihood of electron-hole recombination before they can contribute to the current, thereby reducing J_{sc}. While GaAs initially exhibits higher efficiency, it shows greater sensitivity to defects at higher defect densities, highlighting its vulnerability under such conditions.

III.2.7. Variation of the fill factor (FF) as a function of defect density

Figure 13 shows that GaAs initially exhibits a slightly higher fill factor (FF) compared to BAs; however, both materials experience a similar decline in FF as the defect density increases.

The reduction in FF with increasing defects in the crystalline layer can be attributed to enhanced charge carrier recombination, which decreases the number of carriers available to contribute to the output current. Additionally, some defects may obstruct or scatter incident light, limiting the generation of electron-hole pairs and further contributing to the decline in the fill factor (FF).

III.2.8. Variation of the efficiency (η) as a function of defect density

Figure 14 Initially, BAs exhibits a slightly higher Power Conversion Efficiency (PCE) compared to GaAs; however, both materials show similar declines in PCE as defect density increases.

The fill factor (FF) reflects the efficiency of converting light energy into electricity, accounting for material quality as well as ohmic and recombination

losses. A decrease in FF indicates reduced efficiency, which inevitably lowers the overall performance of the device. Consequently, when FF, J_{sc}, and V_{oc} decline due to crystalline defects, the overall Power Conversion Efficiency (PCE) of the photovoltaic device is significantly impacted.

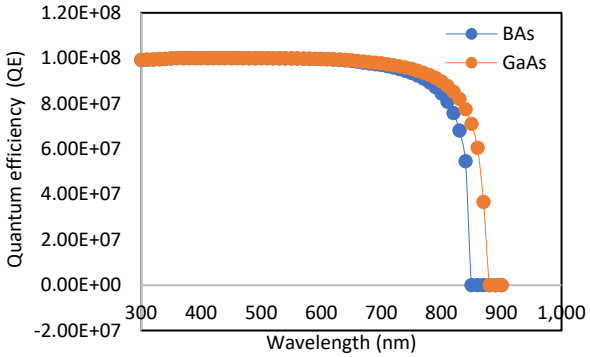

Figure 15. Quantum efficiency of the two structures

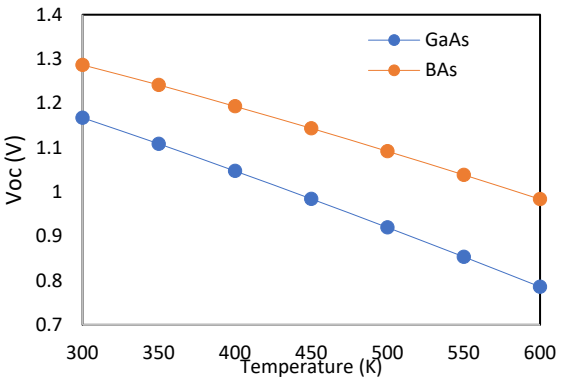

Figure 16. Variation of V_{oc} as a function of temperature

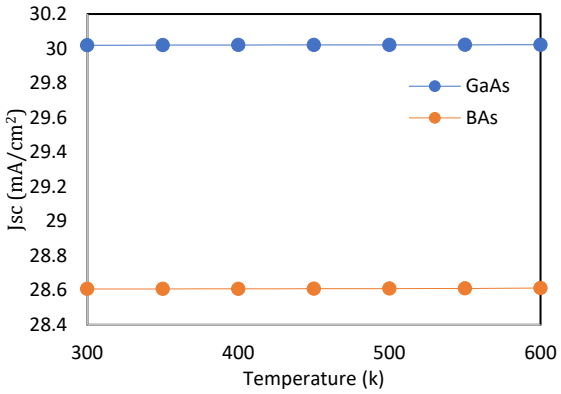

Figure 17. Variation of J_{sc} as a function of temperature

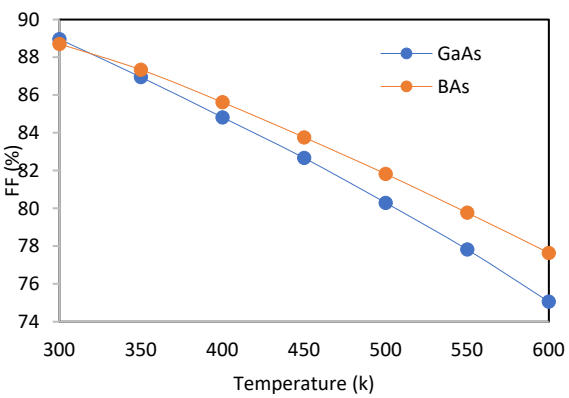

Figure 18. Variation of the fill factor (FF) as a function of temperature

IV. Optimized Configuration

After conducting a series of in-depth analyses on thickness variations, doping, and defects; the optimized solar cell presents a thickness of 0.75µm, a doping concentration of 1E18 cm^{-3}, and a defect density of 1E14 cm^{-3}. This optimization results in an efficiency of 31.17% for the GaAs-based structure and 32.65% for the BAs-based one.

IV.1. Quantum Efficiency

According to Figure 15, GaAs shows a slightly higher quantum efficiency, but the difference is not significant. Both materials are effective over a wide range of wavelengths.

IV. Effect of temperature

After optimizing the photovoltaic cell in terms of active layer thickness, doping, and defect management, it is crucial to study its behavior under extremely high temperature variations. This step allows for the identification of optimal operating conditions to ensure stable and maximum performance, which is essential, particularly for thermophotovoltaic applications, where materials must operate efficiently in extremely high-temperature environments.

IV.1. Effect of temperature on V_{oc}

Figure 16, illustrates a decrease in V_{oc} with increasing temperature for both materials, although BAs consistently maintains a higher value. This suggests superior thermal stability or reduced sensitivity to temperature variations compared to GaAs.

At elevated temperatures, charge carriers gain additional thermal energy, which increases their mobility within the material but reduces the open-circuit voltage. Furthermore, higher temperatures accelerate charge carrier recombination rates, shortening their average lifetime and contributing to the decline in V_{oc}.

IV.2. Effect of temperature on short-circuit current density (J_{sc})

The observations of J_{sc} values as a function of temperature for the two materials (Figure 17) demonstrate a remarkable stability of the short-circuit current density (J_{sc}) as the temperature increases. In the case of GaAs, the values of J_{sc} remain practically constant in the temperature range from 300 K to 500 K, with a slight variation of about 0.0012 mA/cm² over this temperature range. Similarly, for BAs, the J_{sc} values remain stable with a minimal variation of 0.0012 mA/cm² over the same temperature range.

The constancy of J_{sc} (short-circuit current density) shows that temperature does not have a significant impact on short-circuit current generation, confirming good stability in terms of photonic response.

IV.3. Effect of temperature on the fill factor (FF)

Figure 18 shows the evolution of FF as a function of temperature for the two materials: GaAs (Gallium

Arsenide) and BAs (Boron Arsenide). The FF decreases with the increase in temperature for both materials. This indicates that the energy conversion efficiency of devices based on these materials decreases at higher temperatures. This is typical for semiconductor devices because the non-radiative recombination of charge carriers increases with temperature.

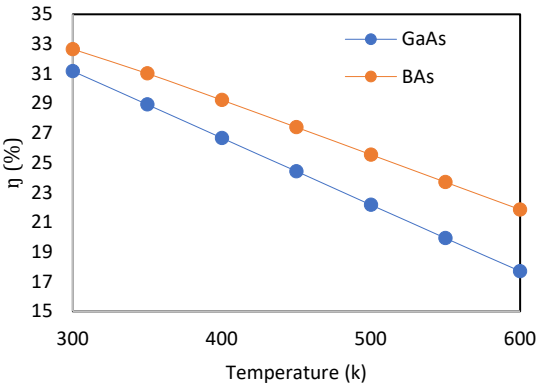

Figure 19. Variation of the efficiency as a function of temperature

IV.4. Effect of temperature on efficiency (ŋ)

Figure 19, presents two graphs showing the efficiency of GaAs and BAs solar cells as a function temperature. The conversion efficiency decreases with the increase in temperature for both materials. Although the short-circuit current (I_{sc}) remains almost stable, the conversion efficiency decreases. This decrease in efficiency can be mainly attributed to a drop in FF and the open-circuit voltage (V_{oc}) with the increase in temperature. The stability of the I_{sc} suggests that photons are still effectively converted into charge carriers, but these charge carriers undergo more non-radiative recombination at higher temperatures. This reduces both V_{oc} and FF, leading to an overall decrease in conversion efficiency.

V. Comparison

Finally, the performance of the two proposed structures, one based on GaAs and the other on BAs, was compared in terms of photovoltaic conversion efficiency (Table 2). This comparison evaluates the effectiveness of both semiconductor materials as active components in solar cells. To contextualize the findings and assess the advancements achieved in this study, the GaAs structure proposed here was also compared with results from previous research (see Table 3).

Table 2. Comparison of photovoltaic performance between GaAs and BAs as an active layer

structures	V_{oc} (V)	J_{sc} (mA/cm^2)	FF (%)	ŋ (%)
Pt/CuO/GaAs/WS2/FTO	1.1738	30.6877	89.27	31.17
Pt/CuO/BAs/WS2/FTO	1.2805	29.2739	88.75	32.65

These results indicate that although GaAs is a high-performance material, BAs offers significant advantages in terms of thermal stability and conversion efficiency, which could make it a promising alternative for high-temperature applications, particularly thermophotovoltaic applications.

Table 3 compares the findings of this study with another similar published research on GaAs. The results demonstrate that our approach achieves strong performance using thinner layers, along with materials that are abundant, easy to fabricate, and less toxic. These attributes contribute to minimizing material waste and promoting environmental sustainability.

Table 3. Comparison of the performance of GaAs-based solar cells with similar studies.

Reference	V_{oc} (V)	J_{sc} (mA/cm^2)	FF (%)	ŋ (%)
Ala'eddin A. Saif, M. Albishri et al (2023) [3]	1.02	47.96	87.48	30.88
This work (2024)	1.1738	30.6877	89.27	31.17

VI. CONCLUSION

This comparative study evaluates the performance of two types of solar cells: one utilizing GaAs and the other BAs. By analyzing a range of performance parameters under comparable conditions, the study identifies the strengths and limitations of each material in photovoltaic applications, paving the way for advancements in solar energy, particularly in thermophotovoltaic technologies.

In this study, we compared the performance of solar cells based on GaAs and BAs using simulations conducted with SCAPS software. The results demonstrated that while GaAs is a well-established material for photovoltaic applications, BAs shows strong potential due to its greater thermal stability, reduced carrier recombination, and higher energy conversion efficiency under specific configurations.

The analysis of key parameters such as open-circuit voltage V_{oc} short-circuit current J_{sc}, fill factor (FF), and conversion efficiency (η) revealed that:

- BAs achieves a higher open-circuit voltage, indicating lower internal energy losses and better charge management.
- GaAs exhibits a slightly higher short-circuit current, likely due to more efficient absorption in the visible spectrum and superior electron mobility.

This study is the first to simulate and compare complete solar cell structures based on GaAs and Bas under an identical architecture, using CuO as the hole transport layer and WS_2 as the electron transport layer, with SCAPS software.

It highlights the promising photovoltaic potential of BAs, identifying optimized configurations (thickness, doping, and defect density) that achieve high efficiencies:

- 31.17% for GaAs
- 32.65% for BAs,

Demonstrating competitive or even superior performance compared to literature reports. The study shows that BAs outperforms GaAs in terms of thermal stability and energy conversion under high-temperature conditions, making it particularly suitable for thermophotovoltaic and space applications.

The analysis is comprehensive, evaluating the impact of multiple parameters on performance (η, Voc, J_{sc}, FF, quantum efficiency), including:

- Active layer thickness
- Doping levels
- Defect density
- Operating temperature

Finally, the study provides practical recommendations for material selection based on target applications:

- GaAs for high-speed conduction solar cells.
- Bas for extreme thermal environments.

This work bridges theoretical insights with practical optimization, advancing the development of next-generation high-efficiency solar cells.

ORCID

Merad Laarej, https://orcid.org/0000-0003-1753-7528; **Mama Bouchaour,** https://orcid.org/0009-0007-3204-0583

REFERENCES

[1] M. Tridane, A. Malaoui, and S. Belaaouad, "Numerical Simulation of pin GaAs Photovoltaic Cell Using SCAPS-1D», Biointerface Research in Applied Chemistry, **13**(4), 253 (2023). https://doi.org/10.33263/BRIAC133.253

[2] A. Kumar, M.S. Thomas, G. Pareek, A. Jain, and N. Gupta, "Performance Evolution of GaAs-Based Solar Cell Towards 30% Efficiency for Space Applications," in: *2022 IEEE International Conference on Nanoelectronics, Nanophotonics, Nanomaterials, Nanobioscience & Nanotechnology (5NANO)*, (IEEE, India, 2022), pp. 1 3. https://doi.org/10.1109/5NANO53044.2022.9828955

[3] M. Burgelman, P. Nollet, and S. Degrave, "Modelling polycrystalline semiconductor solar cells," Thin Solid Films, **361**, 527-532 (2000). https://doi.org/10.1016/S0040-6090(99)00825-1

[4] N. Khoshsirat, N.A.Md. Yunus, "Numerical simulation of CIGS thin film solar cells using SCAPS-1D," in: *2013 IEEE Conference on Sustainable Utilization and Development in Engineering and Technology (CSUDET)*, (Selangor, Malaysia, 2013), pp. 63-67. https://doi.org/10.1109/CSUDET.2013.6670987

[5] R.M. Wentzcovitch, and M.L. Cohen, "Theory of structural and electronic properties of BAs," J. Phys. C Solid State Phys. **19**(34), 6791 (1986). https://doi.org/10.1088/0022-3719/19/34/016

[6] A. Boudjemline, M.M. Islam, L. Louail, and B. Diawara, "Electronic and optical properties of BAs under pressure," Phys. B: Condens. Matter, **406**(22), 4272-4277 (2011). https://doi.org/10.1016/j.physb.2011.08.043

[7] K. Bushick, K. Mengle, N. Sanders, and E. Kioupakis, "Band structure and carrier effective masses of boron arsenide: Effects of quasi-particle and spin-orbit coupling corrections," Appl. Phys. Lett. **114**(2), 022101 (2019). https://doi.org/10.1063/1.5062845

[8] A. Saif, "High-Efficiency homojunction GaAs solar cell using InGaP as FSF and AlGaInP as BSF," Results in Optics, **12**, 100454 (2023). https://doi.org/10.1016/j.rio.2023.100454

[9] K. Ajay, M. S. Thomas, P. Gulshan, A. Jain, et N. Gupta, "Performance Evolution of GaAs-Based Solar Cell Towards >30% Efficiency for Space Applications", IEEE, vol. 1, N° 978, p. 3728-6654. https://doi.org/10.1109/5nano53044.2022.9828955

[9] N. Rono, A.E. Merad, J.K. Kibet, B.S. Martincigh, and V.O. Nyamori, "Optimization of Hole Transport Layer Materials for a Lead-Free Perovskite Solar Cell Based on Formamidinium Tin Iodide," Energy Technol. **9**(12), 2100859 (2021). https://doi.org/10.1002/ente.202100859

[10] S.H. Zyoud, A.H. Zyoud, N.M. Ahmed, R.P. Anupama, S.N. Khan, A.F.I. Abdelkader, and S. Moyad, "Numerical modeling of high conversion efficiency FTO/ZnO/CdS/CZTS/MO thin film-based solar cells: Using SCAPS-1D software," Crystals, **11**(12), 1468 (2021). https://doi.org/10.3390/cryst11121468

[11] J. Shin, G.A. Gamage, Z. Ding, K.E. Chen, F. Tian, X. Qian, J. Zhou, *et al*., "High ambipolar mobility in cubic boron arsenide," Science, **377**(6604), 437-440 (2022). https://doi.org/10.1126/science.abn4290

[12] P.M. Oza, and N.H. Vasoya, "Modeling and simulation of TiO_2/GaAs solar cell using SCAPS", International Journal of Creative Research Thoughts (IJCRT), **10**(12), 2320-2882 (2022). https://www.ijcrt.org/viewfull.php?&p_id=IJCRT2212610

[13] Md.S. Shah, Md.K. Hasan, S.C. Barman, J.A. Bhuiyan, H. Mamur, and M.R. Amin Bhuiyan, "Enhancing PV performance of Al/ZnO/CdS/GaAs/NiO/Au solar cells through diverse layer combinations by SCAPS-1D", Next Research, **2**(1), 100143 (2025). https://doi.org/10.1016/j.nexres.2025.100143

[14] X. Yu, H. He, Y. Hui, H. Wang, X. Zhu, S. Li, and T. Zhu, "Additive engineering for efficient wide-bandgap perovskite solar cells with low open-circuit voltage losses", Frontiers in Chemistry, 12, (2024). https://doi.org/10.3389/fchem.2024.1441057

[15] F.D. Silva, and D.N. Micha, "High-Efficiency GaAs Solar Cell Optimization by Theoretical Simulation", in: *34th Symposium on Microelectronics Technology and Devices (SBMicro)*, (IEEE, Sao-Paulo, Brazil, 2019). https://doi.org/10.1109/SBMicro.2019.8919411

РОЗШИРЕННЯ МЕЖ ЕФЕКТИВНОСТІ: АНАЛІЗ СОНЯЧНИХ ЕЛЕМЕНТІВ GaAs ТА BAs ДЛЯ ФОТОЕЛЕКТРИКИ НАСТУПНОГО ПОКОЛІННЯ НА ОСНОВІ SCAPS

Мерад Лаарей, Мама Бушаур, Іман Буаззауї

Університет Тлемсена, факультет природничих наук, кафедра фізики, дослідницьке об'єднання «Матеріали та відновлювані джерела енергії», URMER BP: 119, Тлемсен, Нуво-Поль, Мансура, 13000, Алжир

У цьому дослідженні використовується програмне забезпечення SCAPS для моделювання та аналізу напівпровідникових матеріалів арсеніду галію (GaAs) та арсеніду бору (BAs) для фотоелектричних застосувань. Ми окреслюємо методологію, підкреслюючи критичні фактори, що враховуються під час моделювання. Продуктивність сонячних елементів досліджується за допомогою кривих квантової ефективності та фотоелектричної продуктивності. Крім того, обговорюються спостережувані тенденції, ключові відмінності між GaAs та BAs, а також їх значення для розвитку високоефективних сонячних елементів.

Ключові слова: *GaAs; BAs; фотоелектрична техніка; програмне забезпечення SCAPS; ефективність перетворення (η)*